GEOLOGY | THE GEOLOGICAL SOCIETY OF AMERICA®

https://doi.org/10.1130/G54254.1

Manuscript received 12 December 2025
Revised manuscript received 18 February 2026
Manuscript accepted 27 February 2026

Published online 19 March 2026

Migrating tremors indicate the activation of distributed melt bodies days before the 2015 Axial Seamount eruption

Juan Zhu[1], Yen Joe Tan[1,*], Yiyuan Zhong[1], Maya Tolstoy[2], Felix Waldhauser[2], and William S.D. Wilcock[3]
[1]Department of Earth and Environmental Sciences, The Chinese University of Hong Kong, Hong Kong SAR, China
[2]Lamont-Doherty Earth Observatory, Columbia University, Palisades, New York 10964, USA
[3]School of Oceanography, University of Washington, Seattle, Washington 98195, USA

ABSTRACT

The traditional view that volcanoes are underlain by a single, melt-dominated magma chamber has recently evolved into the idea that subsurface melt is heterogeneously distributed in a larger magma domain. While seismic imaging of small melt bodies beneath subaerial volcanoes remains difficult, melt bodies located several kilometers from mid-ocean ridge axes and submarine volcanic edifices have been identified. Nevertheless, the connectivity of these melt bodies within the magma domain and their role during eruptions remain unclear. We analyzed continuous ocean-bottom seismic data recorded in 2015–2025 CE that detected 415 volcanic tremor episodes that emerged ~60 h before, and continued during, the 2015 Axial Seamount eruption. The volcanic tremors initiated ~19 km southeast of the caldera before migrating into it and showed spatial overlap with funnel-shaped axial melt lenses and/or lithosphere-asthenosphere boundaries. Our results suggest that these volcanic tremors reflect the activation of or transport through distributed melt bodies over 10 km from the caldera, which provided enhanced magma supply for Axial Seamount's eruption and highlight a broader interconnected active magma plumbing system where melt can be mobilized within a matter of days for an eruption.

INTRODUCTION

Axial Seamount is the most prominent volcanic feature on the Juan de Fuca mid-ocean ridge formed at the intersection with the Cobb-Eickelberg hot spot (northeast Pacific Ocean; Embley et al., 1990; Chadwick et al., 2005). It has experienced three eruptions in the past three decades: in 1998, 2011, and 2015 (Chadwick et al., 2016; Wilcock et al., 2018). It was previously thought that Axial Seamount is underlain by a 14-km-long by 3-km-wide low-seismic-velocity zone at a depth of ~1.5 km below the seafloor (bsf) inferred to represent the main magma reservoir (MMR), with a second low-velocity region inferred to represent a secondary magma reservoir (SMR) located ~5 km to the east based on seismic reflection studies (Fig. 1A) (Arnulf et al., 2014, 2018). More recently, a three-dimensional seismic reflection survey conducted in 2019 over the extended bathymetric plateau of the volcano summit revealed a more accurate estimate of the spatial coverage of the complex magma domain that included funnel-shaped axial melt lenses and/or lithosphere-asthenosphere boundaries (AML|LAB) extending from ~16 km southeast of the caldera, with a maximum depth of ~5–6 km bsf, to ~5 km north of the caldera wall, where the shallowest depth is ~1.1 km bsf (Fig. 1A) (Kent et al., 2025). This structure was inferred to represent a thermally controlled magma assimilation front that focuses magmatism from the off-axis region toward the caldera (Kent et al., 2025). Off-axis melt bodies have also been observed along other mid-ocean ridges such as the East Pacific Rise, the western Galápagos Spreading Center, and Guaymas basin within the Gulf of California through seismic reflection investigations (Lizarralde et al., 2011; Canales et al., 2012; Boddupalli and Canales, 2019). However, it remains unclear how these bodies interconnect to provide melt to the caldera or along the rift zones and whether they actively supply melt during eruptions.

Tremors that occur in volcanic regions are often associated with volcanic unrest and have been used as an important signal for tracking the dynamic processes of magma movement and forecasting volcanic eruptions (Aki and Koyanagi, 1981; Li et al., 2022). The 2015 Axial eruption started at 08:00 UTC on 24 April 2015 and lasted until 21 May 2015 (Nooner and Chadwick Jr., 2016; Caplan-Auerbach et al., 2017). Using the seven Ocean Observatories Initiative (OOI, https://oceanobservatories.org; Kelley et al., 2014) cabled network ocean bottom seismometer (OBS) stations around the southern half of the caldera, Wilcock et al. (2016) manually identified bursts of seismic tremor with strong 7–10 Hz energy in the 6 h before the eruption, but did not locate these events or search for them outside this period. In addition, there have been no further studies of volcanic tremor around Axial Seamount. We systematically detected, located, and characterized volcanic tremors in 2015–2025, which revealed the activation of a broader interconnected magma plumbing system (Sigmundsson, 2016) within a matter of days of the eruption, which presumably provided enhanced magma supply for Axial Seamount's 2015 eruption.

VOLCANIC TREMOR DETECTION, LOCATION, AND FREQUENCY CONTENT CHARACTERIZATION

We first manually checked the 5–30 Hz spectrograms of continuous seismic waveforms recorded by eight OOI stations (seven in the southern half of the caldera, and one southeast of the study area; Fig. 1A) from January to June in 2015 and observed tremor signals with strong energy in 7–15 Hz occurring in the 60 h before and during the 2015 Axial Seamount eruption (Fig. 1B). The tremors were classified into two types: (1) discrete pulsed tremors with multiple individual energy bursts of 8–10 s (Fig. 1C), and (2) continuous tremors with overlapping bursts lasting tens to hundreds of seconds (Fig. 1C).

Yen Joe Tan https://orcid.org/0000-0001-6377-7886
*yjtan@cuhk.edu.hk

CITATION: Zhu, J., et al., 2026, Migrating tremors indicate the activation of distributed melt bodies days before the 2015 Axial Seamount eruption: Geology, v. XX, p. , https://doi.org/10.1130/G54254.1

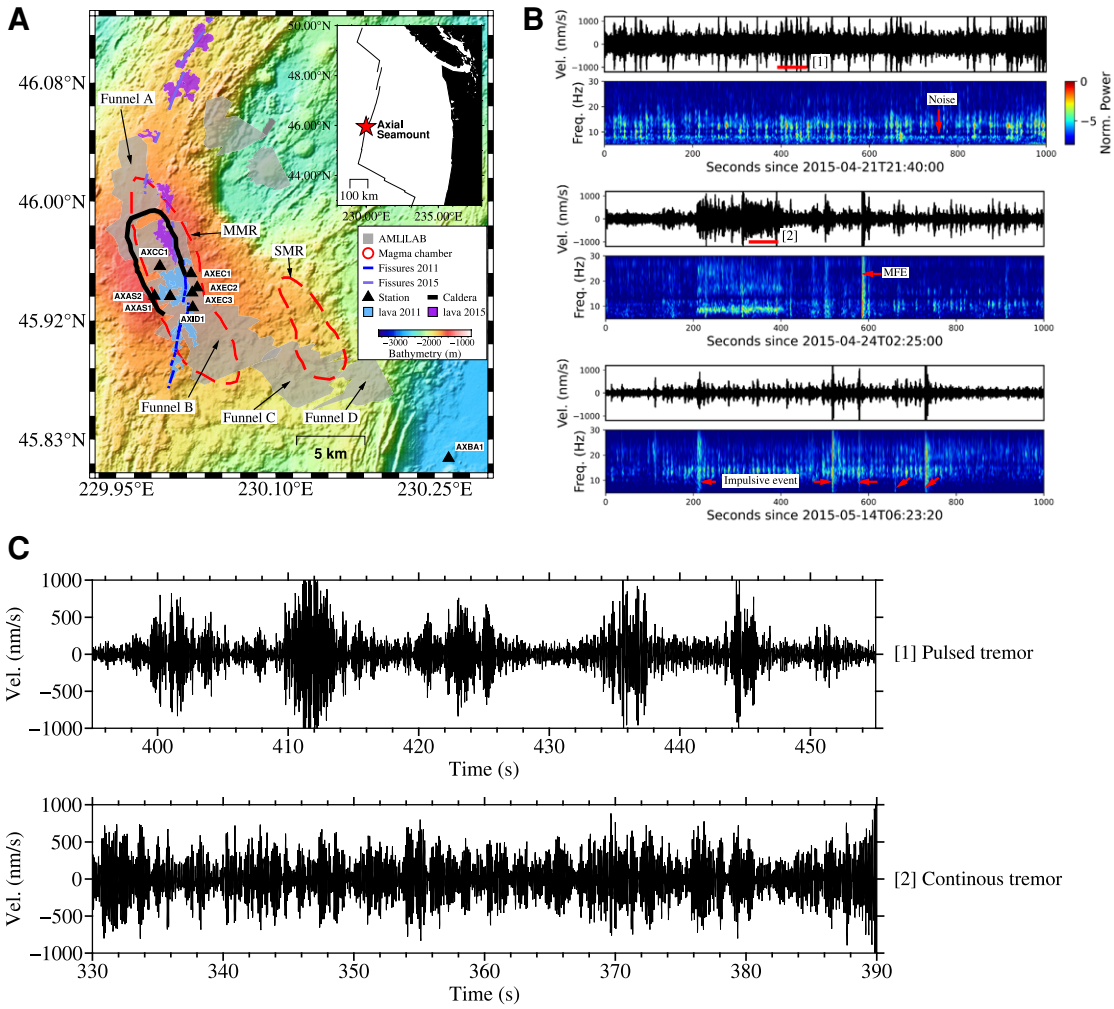

Figure 1. (A) Tectonic setting of Axial Seamount (northeast Pacific Ocean). Black triangles represent eight Ocean Observatories Initiative (https://oceanobservatories.org) ocean bottom seismometer stations, and gray filled regions show axial melt lenses and/or lithosphere-asthenosphere boundary (AML|LAB) funnels imaged by Kent et al. (2025). Red dashed polygons represent the main magma reservoir (MMR) and secondary magma reservoir (SMR) imaged by Arnulf et al. (2018). The black line depicts the Axial Seamount caldera rim. Light-blue and purple filled regions represent erupted lava flows, and blue and dark-purple dashed lines represent eruptive fissures (Chadwick et al., 2016). Background color shows bathymetry (Caress et al., 2012). Inset shows the location of Axial Seamount (red star) relative to plate boundaries (black lines) and land (black shading) in the northeast Pacific Ocean. (B) Three examples of 1000 s velocity seismograms (top) and associated spectrograms (bottom) of tremors at stations AXBA1 (upper), and AXCC1 (middle and bottom). The two red horizontal lines mark the 60 s windows of pulsed and continuous tremors with the enlarged waveforms shown in C). MFE—mix-frequency earthquake; Vel.—velocity; Freq.—frequency; Norm.—normalized. (C) Zoomed-in 60 s velocity seismograms of pulsed tremors in phase 1 (upper) and continuous tremors in phase 2 (bottom).

Similar tremors have also been reported at other volcanoes, such as Whakaari (New Zealand), Fogo (Cape Verde), Tungurahua (Ecuador), and Ruapehu (New Zealand) (Heleno et al., 2006; Bell et al., 2017; Steinke et al., 2024; Bramwell et al., 2025). Thus, we hypothesize that these manually identified seismic tremors are volcanic tremors related to subsurface processes of the magmatic system.

Further analysis was conducted on more than a decade of seismic data recorded by the OOI network (2015–2025) and a temporary OBS deployment (2022–2024) (Fig. 1A; Fig. S1 in the Supplemental Material[1]) to perform detection, location, and frequency content characterization of volcanic tremors around Axial Seamount based on the source characteristics of the manually identified volcanic tremors. The detection and location procedure consisted of three main steps:

1. Obtain a preliminary event catalog of 1 min coherent tremor signals and other types of sources using the waveform envelope correlation and clustering (WECC) method (Wech and Creager, 2008).

2. Remove non-volcanic-tremor sources such as regular earthquakes, mix-frequency earthquakes (MFE), impulsive lava-related seafloor events, T-phase events, air-gun shots, ship noise, and whale calls based on existing catalogs (Le Saout et al., 2020; Wang et al., 2024a, 2024b) and differences in source duration, frequency content, prominent burst peak, and inter-event intervals.

3. Refine the locations of resulting volcanic tremors using a waveform cross-correlation–based method (Obara, 2002) (Text S1). The dominant frequency content of the tremors was defined as the median frequency of the 1 min signal window whose spectral amplitude is sustained at or above 1/3 of the maximum spectral amplitude in 5–30 Hz, averaged across all stations.

CHARACTERISTICS OF THE VOLCANIC TREMORS

A total of 415 1-min volcanic tremor episodes were detected and located around the Axial Seamount. The tremor episodes occur in three different phases, with 146 episodes lasting over 5 h from 20:11 UTC, 2015–04–21, to 01:40 UTC, 2015–04–22 (phase 1); 167 episodes lasting over 14 h from 14:40 UTC, 2015–04–23, to 05:00 UTC, 2015–04–24 (phase 2); and 102 episodes lasting over 14 h from 16:40 UTC, 2015–05–13, to 07:00 UTC, 2015–05–14 (phase 3) (Fig. 2).

Starting ~60 h before the onset of eruption, phase 1 volcanic tremors appeared ~19 km to the southeast of the caldera and migrated northwest toward AML|LAB funnels C and D (Kent et al., 2025; Fig. 3A) with a propagation velocity of ~1.8 km/h (Fig. 3B), which is similar to

[1]Supplemental Material. Volcanic tremor detection and location procedures and uncertainty estimation. Please visit https://doi.org/10.1130/GEOL.S.31434943 to access the supplemental material; contact editing@geosociety.org with any questions.

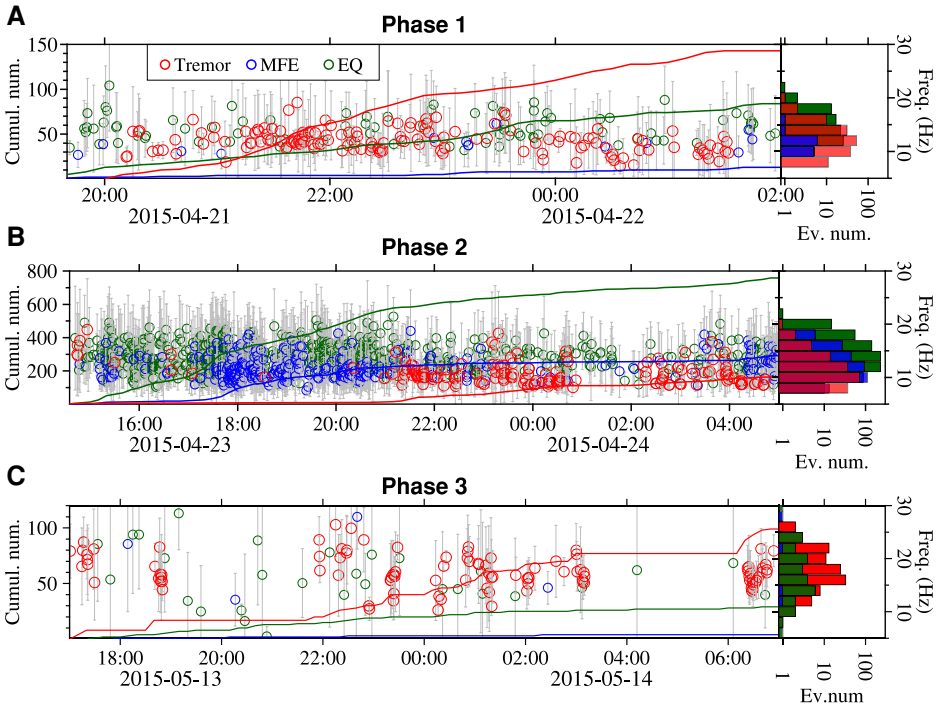

Figure 2. Comparisons of the dominant source frequency of volcanic tremors, mix-frequency earthquakes (MFEs) and regular earthquakes (EQ) in phases 1 (A), 2 (B), and 3 (C) of the 2015 Axial Seamount eruption. Note that the definition used for the dominant source frequency content for each MFE and regular earthquake is the same as for volcanic tremors but with 0.5-s-long waveforms starting from the S-wave arrivals. Volcanic tremors are shown in red, MFEs in blue, and regular earthquakes in green. Lines are the cumulative number (Cumul. num.) of detections (left axis), open circles show the dominant source frequencies, and gray vertical bars represent the standard deviations of the dominant frequency (right axis). Histograms show the dominant frequency of events, with the same color code as in the main figure.

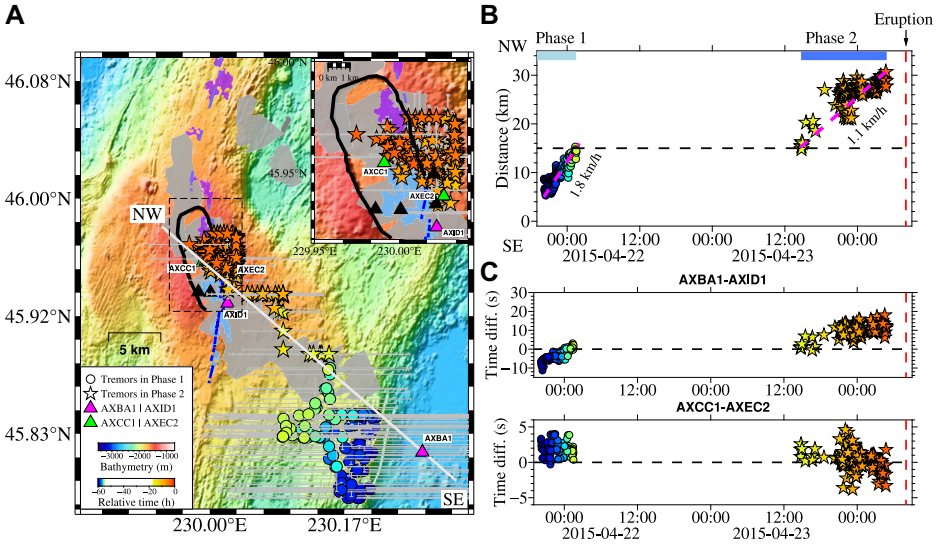

Figure 3. Migration of volcanic tremors before the 2015 Axial Seamount eruption. (A) Spatial distribution of volcanic tremor episodes in phases 1 (circles) and 2 (stars). The horizontal and vertical gray bars represent the uncertainty of volcanic tremor location. The white line represents the southeast-northwest profile shown in B. Other markers are the same as those in Figure 1A. Region inside the black dashed box is shown in the inset. (B) Temporal migration of volcanic tremors along the profile in A, with the dashed magenta lines depicting the migration velocities. (C) Relative arrival time differences between ocean bottom seismometer station pairs for volcanic tremors. Circles and stars in A–C use the same color code for time from eruption onset.

tremor migration velocities during magma intrusions preceding Sierra Negra (Galápagos) and Etna (Italy) eruptions (Saccorotti et al., 2004; Li et al., 2022). During this period, the volcanic tremors overlapped with parts of AML|LAB funnels (Fig. 3A). The volcanic tremor episodes' clear relative arrival time differences between stations (Fig. 3C), and similar spatial migration characteristics when assuming different wave propagation velocities and using different grid search schemes (Text S2; Figs. S12 and S13), suggest that the observed migration pattern is well-constrained. Additionally, phase 1 volcanic tremors exhibited similar frequency content as MFEs previously documented inside Axial caldera and inferred to be associated with influx of magma or volatiles (Wang et al., 2024b), rather than regular earthquakes, which are associated with slip along the caldera ring fault (Wilcock et al., 2016; Wang et al., 2024b) (Fig. 2A); hence, these tremors are likely linked to magma intrusion processes. At ~54 h before the onset of eruption, phase 1 volcanic tremors stopped at the southernmost footprint of the AML|LAB funnel C, ~12 km southeast of the caldera (Fig. 3A), and the quiescence lasted for ~37 h. Hours of seismic quiescence have also been observed at other volcanoes before eruptions, e.g., Telica (Nicaragua) and Sierra Negra, and are linked to the sealing of magma conduits due to mineral deposits, low-porosity magma transport, or crystallization during magma intrusion (Roman et al., 2016; Li et al., 2022).

After the ~37 h of quiescence, phase 2 volcanic tremors emerged ~17 h before the onset of eruption at the same locations as where phase 1 ended (Figs. 2B and 3A). They continued migrating northwest along the southeastern extent of AML|LAB funnels B and C toward the eastern side of the caldera, with a migration velocity of ~1.1 km/h (Figs. 3A and 3B). When the volcanic tremors reached the Axial caldera, they remained around the eastern caldera with a maximum latitude of 45.98°N, showing no further migration northward (Fig. 3A). Additionally, the tremors exhibited similar frequency contents as those in phase 1; hence, are likely indicative of similar magma intrusion processes (Figs. 2A and 2B). At ~3 h before the onset of eruption, the volcanic tremors ended at the eastern side of the Axial caldera. Notably, despite analyzing 10 years of continuous seismic data starting over four months before the eruption, we only detected phase 1 and 2 volcanic tremors starting ~60 h before the eruption.

At ~19 days after the onset of eruption, phase 3 volcanic tremors were concentrated around the central caldera on 13–14 May, which is toward the end of the eruption period, during which there were numerous diffusive events previously interpreted as a type of Hawaiian eruption in the central Axial caldera (Figs. S14a and S14c) (Caplan-Auerbach et al., 2017). The

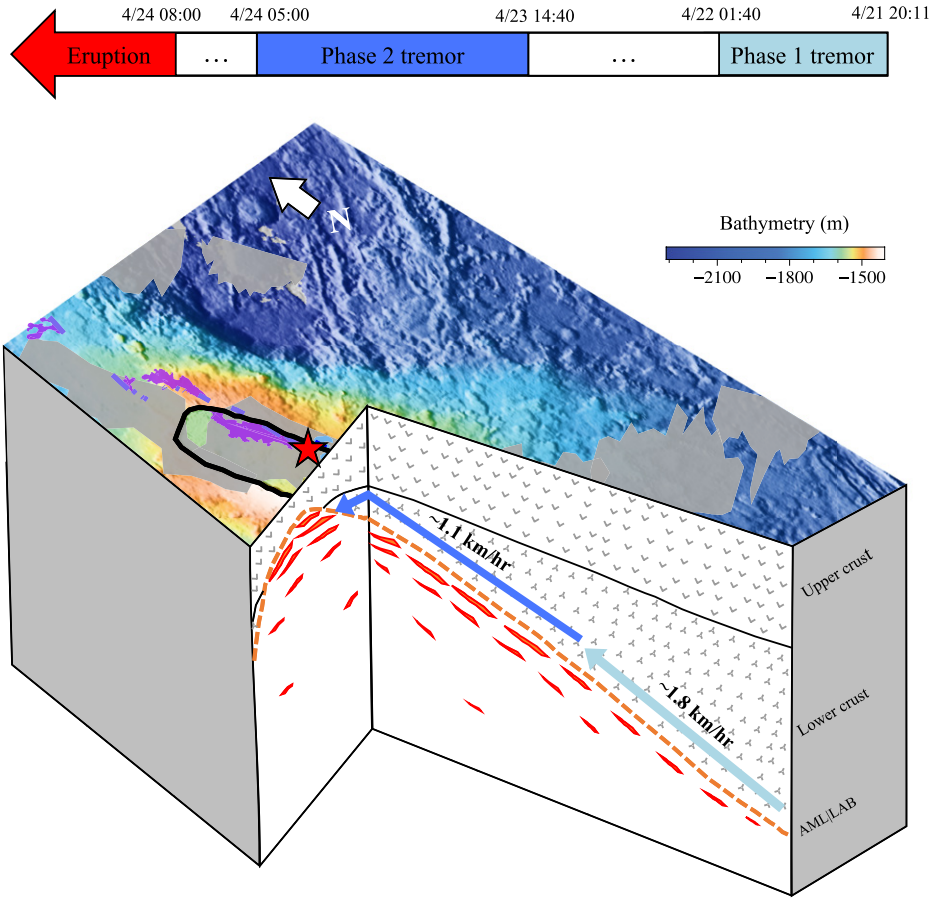

Figure 4. An illustration of the inferred magmatic processes (phases 1 and 2) before the 2015 Axial Seamount eruption. The top left-pointing arrow indicates the timings of tremor occurrence and eruption period. Blue arrows indicate the pre-eruption volcanic tremor migrations. Red filled polygons represent melt lenses. On the seafloor, red star represents where the eruption initiated. Other markers are consistent with those in Figure 1A. AML|LAB—axial melt lenses and/or lithosphere-asthenosphere boundary.

tremors' location in the caldera close to station AXCC1 is well-constrained by the relative arrival times between the stations (Fig. S14b). The volcanic tremors in phase 3 exhibited dominant frequencies of 14–22 Hz (Fig. 2C), in contrast to 7–15 Hz for the phase 1 and 2 volcanic tremors. Therefore, the phase 3 volcanic tremors are inferred to be associated with the Axial eruption rather than magma intrusions.

DISCUSSION AND CONCLUSIONS

In the past decade, there has been a paradigm shift from the traditional view that volcanoes are underlain by a single, melt-dominated magma chamber to the understanding that subsurface melts are distributed more extensively and heterogeneously (Sigmundsson, 2016; Cashman et al., 2017). A high-quality database of volcanic tremors through time may provide insights into the formation, connectivity, and interaction of these distributed melt bodies with main magma reservoirs, as well as their roles during eruptions. At Axial Seamount, a high-quality 3-D seismic reflection survey collected in 2019 (Kent et al., 2025) provided a detailed map of AML|LAB structure, including three AML|LAB funnels (B, C and D) extending ~16 km southeast of the caldera (Fig. 1A). The volcanic tremors we detected show significant spatial overlap with the three AML|LAB funnels ~12 km southeast of the caldera before the eruption (Fig. 3A). Considering the occurrence time, migration pattern, and frequency content of the volcanic tremors, as well as the previous documentation of high CO_2 content in basaltic glasses from Axial Seamount (Figs. 2 and 3A) (Dixon et al., 1988), we infer that the volcanic tremors indicate activation of or transport through distributed melt bodies in the off-axis regions preceding the eruption, with the detected tremors potentially linked to CO_2 slug releases during magma intrusions (Fig. 4) (Steinke et al., 2024; Bramwell et al., 2025). Our results not only support Kent et al.'s (2025) hypothesis that these distributed melt bodies provide enhanced magma supply for Axial's eruption but also illuminate the subcaldera MMR's connectivity with a wider network of melt bodies that can feed the caldera within a matter of days (Figs. 3A and 4). This precursory activation of a broader, distributed magmatic system further suggests that magma overpressure was the dominant driver behind the 2015 Axial Seamount eruption, which differs from non-hotspot–influenced mid-ocean ridges like the East Pacific Rise and the Endeavor segment where build-up of tectonic extensional stress serves as the primary driver of eruptions (Tan et al., 2016; Krauss et al., 2023).

Volcanic tremors have been reported in some volcanic regions, e.g., at Etna and Stromboli, in the days to hours before eruptions (Ripepe et al., 2009; Langer et al., 2022). Dramatic changes in seafloor deformation and increases in MFEs and regular earthquake activities were observed in the days to months before the 2015 Axial eruption (Nooner and Chadwick Jr., 2016; Wilcock et al., 2016; Wang et al., 2024b). These changes could serve as valuable precursors for forecasting eruptions at Axial Seamount. However, forecasting on short time scales remains challenging for Axial's eruption. For example, MFEs occurred in large numbers ~15 h prior to the 2015 eruption, but low-level MFE activity is also observed in other time periods, with a steady increase in the months prior to the eruption (Fig. 2) (Wang et al., 2024b). In comparison, when searching through OBS data across a 10-yr period, we identified volcanic tremors that only appeared ~60 h before, and continued during, the eruption (Fig. 2). Therefore, these volcanic tremors have the potential to enhance short-term forecasting for future Axial eruptions assuming that eruptions at Axial are characteristic. Additionally, the southeasternmost volcanic tremors do not fully overlap with the funnel-shaped AML|LAB structures, which could be due to location uncertainties of the tremors in the longitudinal direction (Fig. 3A) or the spatial limit and timing (~4 years after the eruption) of the active source survey (Kent et al., 2025). Extending the deployment of seismic stations to the southeast of the Axial caldera would help us better understand active processes related to the wider interconnected magma plumbing system.

ACKNOWLEDGMENTS

We thank editor Scott King, Graham Kent, and an anonymous reviewer for their constructive reviews, which have significantly improved the paper. We also thank Kaiwen Wang and Peifeng Wang for helpful suggestions. This work received support from the Hong Kong Research Grants Council General Research Fund (grant 14300422), the Chinese University of Hong Kong Postdoctoral Fellowship Scheme (grant 3135127), the Croucher Tak Wah Mak Innovation Award, and the National Science Foundation Fund (grant NSF-OCE 1951448).

REFERENCES CITED

Aki, K., and Koyanagi, R., 1981, Deep volcanic tremor and magma ascent mechanism under Kilauea, Hawaii: Journal of Geophysical Research: Solid Earth, v. 86, p. 7095–7109, https://doi.org/10.1029/JB086iB08p07095.

Arnulf, A., Harding, A., Kent, G., Carbotte, S., Canales, J., and Nedimović, M., 2014, Anatomy

of an active submarine volcano: Geology, v. 42, p. 655–658, https://doi.org/10.1130/G35629.1.
Arnulf, A., Harding, A., Kent, G., and Wilcock, W., 2018, Structure, seismicity, and accretionary processes at the hot spot-influenced Axial Seamount on the Juan de Fuca Ridge: Journal of Geophysical Research: Solid Earth, v. 123, p. 4618–4646, https://doi.org/10.1029/2017JB015131.
Bell, A.F., Hernandez, S., Gaunt, H.E., Mothes, P., Ruiz, M., Sierra, D., and Aguaiza, S., 2017, The rise and fall of periodic 'drumbeat' seismicity at Tungurahua volcano, Ecuador: Earth and Planetary Science Letters, v. 475, p. 58–70, https://doi.org/10.1016/j.epsl.2017.07.030.
Boddupalli, B., and Canales, J., 2019, Distribution of crustal melt bodies at the hot spot-influenced section of the Galápagos Spreading Centre from seismic reflection images: Geophysical Research Letters, v. 46, p. 4664–4673, https://doi.org/10.1029/2019GL082201.
Bramwell, L.A., Illsley-Kemp, F., Hughes, E.C., Butcher, S., Lamb, O.D., and Behr, Y., 2025, Source dynamics of Ruapehu's 2022 volcanic unrest: Insights from drumbeat seismicity, tremor, and crater lake signals: Bulletin of Volcanology, v. 87, 44, https://doi.org/10.1007/s00445-025-01823-2.
Canales, J., Carton, H., Carbotte, S., Mutter, J., Nedimović, M., Xu, M., Aghaei, O., Marjanović, M., and Newman, K., 2012, Network of off-axis melt bodies at the East Pacific Rise: Nature Geoscience, v. 5, p. 279–283, https://doi.org/10.1038/ngeo1377.
Caplan-Auerbach, J., Dziak, R., Haxel, J., Bohnenstiehl, D., and Garcia, C., 2017, Explosive processes during the 2015 eruption of Axial Seamount, as recorded by seafloor hydrophones: Geochemistry, Geophysics, Geosystems, v. 18, p. 1761–1774, https://doi.org/10.1002/2016GC006734.
Caress, D.W., Clague, D.A., Paduan, J.B., Martin, J.F., Dreyer, B.M., Chadwick, W.W., Jr., Denny, A., and Kelley, D.S., 2012, Repeat bathymetric surveys at 1-metre resolution of lava flows erupted at Axial Seamount in April 2011: Nature Geoscience, v. 5, p. 483–488, https://doi.org/10.1038/ngeo1496.
Cashman, K.V., Sparks, R.S.J., and Blundy, J.D., 2017, Vertically extensive and unstable magmatic systems: A unified view of igneous processes: Science, v. 355, https://doi.org/10.1126/science.aag3055.
Chadwick, J., Perfit, M., Ridley, I., Jonasson, I., Kamenov, G., Chadwick, W., Embley, R., Le Roux, P., and Smith, M., 2005, Magmatic effects of the Cobb hot spot on the Juan de Fuca Ridge: Journal of Geophysical Research: Solid Earth, v. 110, B03101, https://doi.org/10.1029/2003JB002767.
Chadwick, W.W., Jr., Paduan, J., Clague, D., Dreyer, B., Merle, S., Bobbitt, A., Caress, D., Philip, B., Kelley, D., and Nooner, S., 2016, Voluminous eruption from a zoned magma body after an increase in supply rate at Axial Seamount: Geophysical Research Letters, v. 43, p. 12,063–12,070, https://doi.org/10.1002/2016GL071327.
Dixon, J.E., Stolper, E., and Delaney, J.R., 1988, Infrared spectroscopic measurements of CO_2 and H_2O in Juan de Fuca Ridge basaltic glasses: Earth and Planetary Science Letters, v. 90, p. 87–104, https://doi.org/10.1016/0012-821X(88)90114-8.
Embley, R.W., Murphy, K.M., and Fox, C.G., 1990, High-resolution studies of the summit of Axial Volcano: Journal of Geophysical Research: Solid Earth, v. 95, B8, p. 12,785–12,812, https://doi.org/10.1029/JB095iB08p12785.
Heleno, S.I., Faria, B.V., Bandomo, Z., and Fonseca, J.F., 2006, Observations of high-frequency harmonic tremor in Fogo, Cape Verde Islands: Journal of Volcanology and Geothermal Research, v. 158, p. 361–379, https://doi.org/10.1016/j.jvolgeores.2006.06.018.
Kelley, D.S., Delaney, J.R., and Juniper, S.K., 2014, Establishing a new era of submarine volcanic observatories: Cabling Axial Seamount and the Endeavour Segment of the Juan de Fuca Ridge: Marine Geology, v. 352, p. 426–450, https://doi.org/10.1016/j.margeo.2014.03.010.
Kent, G., Arnulf, A., Singh, S., Carton, H., Harding, A., and Saustrup, S., 2025, Melt focusing along lithosphere–asthenosphere boundary below Axial volcano: Nature, v. 641, p. 380–387, https://doi.org/10.1038/s41586-025-08865-8.
Krauss, Z., Wilcock, W.S., Heesemann, M., Schlesinger, A., Kukovica, J., and Farrugia, J.J., 2023, A long-term earthquake catalog for the Endeavour segment: Constraints on the extensional cycle and evidence for hydrothermal venting supported by propagating rifts: Journal of Geophysical Research: Solid Earth, v. 128, https://doi.org/10.1029/2022JB025662.
Langer, H., Falsaperla, S., Spampinato, S., and Messina, A., 2022, Energy threshold changes in volcanic activity at Mt. Etna (Italy) inferred from volcanic tremor: Scientific Reports, v. 12, 17895, https://doi.org/10.1038/s41598-022-20766-8.
Le Saout, M., Bohnenstiehl, D., Paduan, J., and Clague, D., 2020, Quantification of eruption dynamics on the north rift at Axial Seamount, Juan de Fuca Ridge: Geochemistry, Geophysics, Geosystems, v. 21, https://doi.org/10.1029/2020GC009136.
Li, K.L., Bean, C.J., Bell, A.F., Ruiz, M., Hernandez, S., and Grannell, J., 2022, Seismic tremor reveals slow fracture propagation prior to the 2018 eruption at Sierra Negra volcano, Galápagos: Earth and Planetary Science Letters, v. 586, https://doi.org/10.1016/j.epsl.2022.117533.
Lizarralde, D., Soule, S.A., Seewald, J.S., and Proskurowski, G., 2011, Carbon release by off-axis magmatism in a young sedimented spreading centre: Nature Geoscience, v. 4, p. 50–54, https://doi.org/10.1038/ngeo1006.
Nooner, S.L., and Chadwick, W.W., Jr., 2016, Inflation-predictable behavior and co-eruption deformation at Axial Seamount: Science, v. 354, p. 1399–1403, https://doi.org/10.1126/science.aah4666.
Obara, K., 2002, Nonvolcanic deep tremor associated with subduction in southwest Japan: Science, v. 296, p. 1679–1681, https://doi.org/10.1126/science.1070378.
Ripepe, M., Delle Donne, D., Lacanna, G., Marchetti, E., and Ulivieri, G., 2009, The onset of the 2007 Stromboli effusive eruption recorded by an integrated geophysical network: Journal of Volcanology and Geothermal Research, v. 182, p. 131–136, https://doi.org/10.1016/j.jvolgeores.2009.02.011.
Roman, D.C., Rodgers, M., Geirsson, H., LaFemina, P.C., and Tenorio, V., 2016, Assessing the likelihood and magnitude of volcanic explosions based on seismic quiescence: Earth and Planetary Science Letters, v. 450, p. 20–28, https://doi.org/10.1016/j.epsl.2016.06.020.
Saccorotti, G., Zuccarello, L., Del Pezzo, E., Ibanez, J., and Gresta, S., 2004, Quantitative analysis of the tremor wavefield at Etna Volcano, Italy: Journal of Volcanology and Geothermal Research, v. 136, p. 223–245, https://doi.org/10.1016/j.jvolgeores.2004.04.003.
Sigmundsson, F., 2016, New insights into magma plumbing along rift systems from detailed observations of eruptive behavior at Axial volcano: Geophysical Research Letters, v. 43, p. 12,423–12,427, https://doi.org/10.1002/2016GL071884.
Steinke, B., Jolly, A., Girona, T., Caudron, C., Bramwell, L., Cronin, S., Illsley-Kemp, F., and Hughes, E., 2024, Dynamics and detection of pulsed tremor at Whakaari (White Island), Aotearoa New Zealand: Geophysical Research Letters, v. 51, https://doi.org/10.1029/2024GL110447.
Tan, Y.J., Tolstoy, M., Waldhauser, F., and Wilcock, W.S., 2016, Dynamics of a seafloor-spreading episode at the East Pacific Rise: Nature, v. 540, p. 261–265, https://doi.org/10.1038/nature20116.
Wang, K., Waldhauser, F., Schaff, D., Tolstoy, M., Wilcock, W.S., and Tan, Y.J., 2024a, Real-time detection of volcanic unrest and eruption at Axial Seamount using machine learning: Seismological Research Letters, v. 95, p. 2651–2662, https://doi.org/10.1785/0220240086.
Wang, K., Waldhauser, F., Tolstoy, M., Schaff, D., Sawi, T., Wilcock, W.S., and Tan, Y.J., 2024b, Volcanic precursor revealed by machine learning offers new eruption forecasting capability: Geophysical Research Letters, v. 51, https://doi.org/10.1029/2024GL108631.
Wech, A.G., and Creager, K.C., 2008, Automated detection and location of Cascadia tremor: Geophysical Research Letters, v. 35, https://doi.org/10.1029/2008GL035458.
Wilcock, W.S., Dziak, R.P., Tolstoy, M., Chadwick, W.W., Jr., Nooner, S.L., Bohnenstiehl, D.R., Caplan-Auerbach, J., Waldhauser, F., Arnulf, A.F., and Baillard, C., 2018, The recent volcanic history of Axial Seamount: Geophysical insights into past eruption dynamics with an eye toward enhanced observations of future eruptions: Oceanography, v. 31, p. 114–123, https://doi.org/10.5670/oceanog.2018.117.
Wilcock, W.S., Tolstoy, M., Waldhauser, F., Garcia, C., Tan, Y.J., Bohnenstiehl, D.R., Caplan-Auerbach, J., Dziak, R.P., Arnulf, A.F., and Mann, M.E., 2016, Seismic constraints on caldera dynamics from the 2015 Axial Seamount eruption: Science, v. 354, p. 1395–1399, https://doi.org/10.1126/science.aah5563.

Printed in the USA